A 3D-DEM Model for Tropical Residual Soils Under Monotonic and Cyclic Loadings

Tarek Mohamed, Jérôme Duriez, Guillaume Veylon, L. Peyras, P. Soulat

A 3D-DEM Model for Tropical Residual Soils Under Monotonic and Cyclic Loadings

T. Mohamed[1], J. Duriez[2], G. Veylon[3], L. Peyras[4], and P. Soulat[5]

[1]INRAE, Aix Marseille Univ, RECOVER, Aix-en-Provence, France
[2]INRAE, Aix Marseille Univ, RECOVER, Aix-en-Provence, France, Email: jerome.duriez@inrae.fr
[3]INRAE, Aix Marseille Univ, RECOVER, Aix-en-Provence, France
[4]INRAE, Aix Marseille Univ, RECOVER, Aix-en-Provence, France
[5]Suez Consulting, Safege, Montpellier, France

ABSTRACT

Tropical residual soils are found in different parts of the world and consist of mixtures of different types of soil such as sand, silt and clay, resulting in intricate microstructures and mechanical responses. In this context and inspired by the soil's composition, a 3D-DEM model is developed in which two different contact models are assigned among idealized spherical particles to represent the coarse and fine parts of the tropical soil with two distinct sets of numerical parameters. A simple linear rolling resistance contact model is used to represent the coarse, cohesionless, component, while a softer adhesive rolling resistance contact model with a linear approximation of the van der Waals attraction force is used for the fine, cohesive, component. The numerical coarse network is continuous in terms of interparticle contacts and represents the main skeleton of the DEM sample, whereas so-called fine contacts form a local force network between the coarse particles. After a parametric study on the effects of adopting such a numerical mixture, the model is calibrated for a drained compression triaxial test with a specific void ratio. In order to estimate the equivalent DEM model void ratio, a proportionality between the real soil void ratio and the DEM model void ratio

is efficiently employed. During the validation phase, successful model predictions are achieved on drained and undrained triaxial tests and cyclic tests with different strain amplitudes and moderate (hundreds of kPa) confining pressures.

PRACTICAL APPLICATIONS

Tropical residual soils are proposed to be simulated through a grain-based numerical model using the Discrete Element Method, being inspired from the microstructure and the physical components of those soils. The proposed model may contribute to reliable numerical modeling of existing or new earthfill structures under monotonic and cyclic loadings in tropical areas in a diverse manner. First, with an understanding of its limitations, e.g., regarding grain breakage, the model can complement lab mechanical tests, which are often scarce, to consider additional loading conditions. Doing so, it may inspire a better definition of analytical constitutive relations for tropical soils since the model outputs a wide range of macro- and micro-scale information, e.g., elastic properties, the influence of the fine content, etc., on the mechanical behavior of mixed soils. Finally, with significant computational resources, it could be directly employed for 3D multi-scale discrete-continuum modeling of a structure as a boundary value problem, whereby analytical constitutive models are bypassed and the constitutive response of the material is instead derived through direct stress-strain computations in the proposed model.

INTRODUCTION

Tropical residual soils appear in different places over the world and can be used in different geotechnical structures such as earthfill dams. They are formed by the process of in-situ chemical weathering of a parent rock under humid tropical conditions. Tropical residual soils present very specific properties due to the resulting physico-chemical composition (Futai et al. 2004; Futai and Almeida 2005; Lopes et al. 2022; Mouali 2021). Depending on the weathering grade, residual soils may preserve macrostructure inherited from the parent rock as well as its microstructure in terms of fabric, pores and bonds between soil aggregates. Moreover, the composition of the tropical soil of different types of soils such as sand, silt and clay induces a complex mechanical response that requires an advanced numerical model able to take into account the effect and the evolution of the different ingredients on the mechanical behavior. The features of elasto-plastic models developed so far to model the behavior of residual soils (Mendoza and de Farias 2020) are not sufficient to model their cyclic behavior, in particular because they do not take into account the effect of the evolutions of the microstructure and of inter-granular bonding during loading-unloading paths.

On the other hand, the DEM approach has been widely used to simulate the mechanical behavior of granular materials over the last several decades, demonstrating a high capability to reproduce the different characteristics of sand under monotonic (Hosn et al. 2017; Sibille et al. 2019; Karapiperis et al. 2020; Mohamed et al. 2022) and cyclic loadings (Wang et al. 2016; Gu et al. 2020). Previous DEM (Gong et al. 2019) and experimental (Yang and Liu 2016) studies of granular mixtures demonstrate the effect of fine content on the soil mechanical response by which maximum shear modulus G_0 decreases with increasing fine contents F_C. They have shown how a higher $\alpha = D_c/D_f$ ratio (D_c and D_f are the sizes of coarse and fine particles) helps fine particles to occupy voids between coarse particles. Gong et al. (2019) uses size ratio $\alpha = 5$ to study the effect of a moderate fine content $F_c \leq 20\%$ on the mechanical behavior of natural sand. Compared with other DEM simulations, Shire et al. (2016) adopts a higher value, $\alpha = 6 - 10$, during his DEM simulation of gap-graded soil. The general conclusion of the latter studies is that as α increases, fine particles are able to fit more efficiently within voids between coarse particles without significantly disturbing the main skeleton formed by coarse particles.

Cohesive soils have been studied by the DEM approach (Tsuji et al. 2012; Gu et al. 2016; Li et al. 2018) much less frequently than cohesion-less ones. The existing applications of the DEM method to complex in-situ or mixed soils are thus limited so far in spite of its capabilities to reproduce mechanically important microstructural phenomena that also exist in clayey soils, such as aggregate orientation (Hattab and Fleureau 2011).

As such, taking a step further and simulating mixed soils is the concern of this study. Namely, this article presents a quantitative modeling approach for the mechanical behavior of tropical soils, by applying the DEM approach to a tropical soil found in Guadeloupe, France, which is a highly seismic zone posing clear challenges to geotechnical engineering. As it will be shown, such a mixed soil requires different contact models to reflect the different evolution logic of the different components of the tropical soil in addition to the preceding needs of particle size considerations. Inspired by the existing mixture of sand, silt, and clay and the microstructure of tropical soils, the DEM model will contain a mixture of so-called coarse and fine contacts by using a sample with two different contact models (cohesive and non-cohesive contact models) to reflect and simulate the effect of the fine and coarse materials of the tropical soil on the mechanical response. The simulations are performed using the commercial software PFC (Itasca 2018).

The article consists of three main sections. The first section describes the general formulation of the 3D-DEM model with its two contact models and a wide particle distribution, which is inspired by the physical characteristics of the studied tropical soil from Guadeloupe. The second section presents a parametric study on the effect of different contact mixtures and contact parameters, as well as the model calibration procedure. Finally, we provide the validation results for the DEM model under different loading paths, including monotonic (oedometer tests, drained and undrained triaxial compression) and cyclic (undrained triaxial tests) loadings for different values of initial void ratio and confining pressure.

GENERAL FORMULATION OF THE DEM MODEL FROM SOIL CHARACTERISTICS

Physical characteristics of tropical residual soil

Tropical soil samples have been collected in (Mouali 2021; Suez Consulting 2016) from the construction site of an earth dam in the French West Indies (Guadeloupe). The representative grain size distribution is shown in Fig. 1 together with a plasticity chart. The soil contains around 50% of clay, 25% of silt and 25% of sand-sized particles. The clay minerals contain kaolinite and halloysite in a random contact state. The liquid limit is (62-73%) and the plasticity index is $I_p = 12 - 27\%$ corresponding to non-plastic silts. The average value of the specific gravity of soil grains, Gs, is 2.71. While the particle size distribution could naturally vary with the extraction depth and from one location to another, it has been checked that the different experimental sources used here for this site (Mouali 2021; Suez Consulting 2016; Mouali et al. 2019) share nearly the same granulometry as previously described.

Model formulation from a wide particle size distribution and different contact models

For the purpose of DEM modeling, spherical particle shapes bounded with rigid walls are considered for computational simplicity since this assumption enables simulations to run approximately 10 to 100 times faster (Duriez and Bonelli 2021; Mohamed et al. 2022) on a given hardware. The REV with a number of 5100 particles is used for the current DEM model. As was proven (Mohamed et al. 2022) for a similar sample preparation method it is sufficient to give a uniform distribution of porosity inside a DEM sample and an unaffected stress-strain response when the number of particles exceeds this value. While it would be impossible to replicate in the DEM model the several decades-wide particle size distribution of the real soil in Fig. 1, a large $\frac{D_{max}}{D_{min}} = 10$ maximum-to-minimum particle size ratio is still set in this study for the 3D-DEM particle size distribution model, see Table 2 and Fig. 2. This ensures the possibility of having small particles occupy the voids between the coarse particles, likewise to the real soil, which is successfully achieved as shown in Fig. 2.

As another key ingredient of the model, particles interaction is herein described through two different contact models already implemented in the PFC software (Itasca 2018) and which are used to reflect the different physics of the granular and cohesive ingredients of the tropical soil. Fig. 3 illustrates the micro-scale interpretation of using different contact models in the DEM model.

As for the granular part, a classical rolling resistance contact model is used. It first includes an elastic normal contact force $\vec{f_n}$ being defined as follows:

$$\vec{f_n} = K_n \vec{\delta}_n \tag{1}$$

$$K_n = E_{mod} \frac{\pi r^2}{R_1 + R_2} \; with \; r = min(R_1, R_2) \tag{2}$$

where $\vec{\delta}_n$ is the relative normal-displacement parallel to the contact normal $\vec{n}_c$ and K_n is the normal stiffness being a function of a stress-like parameter E_{mod} together with R_1 and R_2 the radii of the two contacting spheres. In addition, a shear force is updated incrementally as follows:

$$\vec{f_s} = \vec{f_s^0} + K_s \Delta\vec{\delta}_s \tag{3}$$

where $\vec{f_s^0}$ is the shear force at the beginning of a time step and K_s the contact tangential stiffness. Eq. (3) holds until a Coulomb friction condition is imposed to limit the shear force of the contact as follows:

$$||\vec{f_s}|| \leq ||\vec{f_n}||\mu \tag{4}$$

where μ is the coefficient of friction at the contact level. The contact model finally includes interparticle torques or moments that resist relative rolling, as per the following rolling stiffness and moment incremental laws:

$$K_r = K_s R_m^2 \tag{5}$$

$$\frac{1}{R_m} = \frac{1}{R_1} + \frac{1}{R_2} \tag{6}$$

$$\Delta\vec{M}_r = K_r \Delta\vec{\theta}_b \;\; ||\vec{M}_r|| \leq \mu_r ||\vec{f_n}|| R_m \tag{7}$$

$$\Delta\vec{\theta}_b = \Delta\vec{\theta} - \Delta\theta_t \vec{n}_c \tag{8}$$

where μ_r, R_m, $\Delta\vec{\theta}$, $\Delta\vec{\theta}_b$ and $\Delta\theta_t$ are defined as the rolling friction coefficient, effective radius, rotation increment, relative bend-rotation increment and the relative twist-rotation increment respectively.

For describing the fine component of the tropical soil, an adhesive rolling resistance linear model (Gilabert et al. 2007) is used with attractive forces that are responsible for the cohesion of the material and the existence of macroporous (inter-particles) microstructures in fine-grained soils (Li et al. 2018; Sun et al. 2018). The adhesive rolling contact model, illustrated in Fig. 4, adds a cohesive component to the above rolling resistance contact model via a linear approximation of van der Waals attraction force (electrostatic forces) within an attraction range (0 - D_0) for the gap distance between two grains, g_s. The attractive force F^a is maximum, equal to F_0, when g_s has negative values as shown in Fig. 4. In between $g_s \geq 0$ and $g_s = D_0$ the adhesive force is updated as follows:

$$F^a = \begin{cases} F_0, & g_s \leq 0 \\ F_0\left(1 - \frac{g_s}{D_0}\right), & 0 < g_s < D_0 \\ 0, & g_s \geq D_0. \end{cases} \tag{9}$$

Despite the fact that actual van der Waals forces exist on a smaller scale for tropical soil clay particles than for DEM particles, this concept can introduce a soft behavior for the cohesive force and prevents brittle failure at the level of contacts that can happen in the case of the classical linear contact bond model with a constant cohesive parameter (bonded or unbonded interface), which is more suited to materials such as concrete and rocks (Potyondy and Cundall 2004). It is also worth mentioning that the attraction force parameter F_0 is directly input as a force quantity by the user, instead of adopting an adhesive rolling resistance model that would be normalized according to the dimension of particles. As a result, the cohesive strength of the sample is proportional to the size of particles contained within the packing making particles' absolute diameters part of model parameters (Table 2). The total contact force F_c of the adhesive contact model is eventually described as follows:

$$\vec{F_c} = \vec{F^l} + \vec{F^{adh}}, \qquad \vec{F^{adh}} = -F^a \vec{n}_c \tag{10}$$

where $\vec{F^l} = \vec{f_n} + \vec{f_s}$ and $\vec{F^{adh}}$ represent linear and adhesive forces respectively.

These two key model ingredients (the particle size distribution and the use of two different contact models) are unrelated in the sense that attributing one or another contact model to a particle pair does not follow particle size considerations but instead derives from a specific packing preparation phase, described below.

Preparation of numerical samples

The preparation phase (under no gravity) is responsible for specifying heterogeneity in contact model properties and controlling, to a desired value, the proportion between the so-called fine contacts following the adhesive contact model and those that will follow the simple rolling resistance contact model and account for the coarse component of the soil.

The procedure actually relies on an ad-hoc initial generation of the packing (obeying the granulometry discussed above) where a controlled number of spheres overlap. Then, DEM cycles are performed to bring the model to equilibrium under zero external stress (almost no internal contact). At this stage, all active contacts (very few contacts) and inactive contacts (an inactive contact refers to a pair of particles which have been touching previously but no longer do) are registered and they directly define the list of all possible coarse contacts which will be assigned the rolling resistance contact model in case these contacts would later reform. Through controlling the number of overlaps at the very initial stage, this process enables to control the proportion of the coarse component to be simulated (the more the overlap, the more important the coarse phase), as shown in Fig. 5.

So-called fine contacts following the adhesive rolling resistance contact model will then appear during the subsequent simulation stages (starting with the confining phase), through any new contact which would not be part of the above list. It is to recall the definition of a fine contact does not follow particle size considerations and may also apply between small and big spheres as shown in Fig. 3. The portion of each contact model in the global force network is separated and shown in Fig. 6 where it clearly appears that the main skeleton of the sample is formed by the coarse contacts and that the fine contacts form less continuous force networks which represent the trapped fine particles within the main skeleton.

Heterogeneity in contact properties is further enhanced by applying two distinct sets of numerical parameters in the common portion of the contact models, with a lower modulus E_{mod} and a lower rolling friction coefficient μ_r for the so-called fine contacts, as it will be shown in more details in the forthcoming calibration phase

Regarding the packing properties, the anisotropy of the sample is important in DEM simulations, as highlighted e.g. by Mohamed et al. (2022), and is herein quantified as an anisotropy scalar A for the fabric tensor F_{ij}, which is defined as the ratio between the norm of the deviatoric part of the fabric tensor and one-third of the first invariant of the fabric tensor. By taking into account the axisymmetric condition of the triaxial test around axis Z and the principal nature of axes X, Y, Z, the equation yields to:

$$A = \frac{3(F_{ZZ} - F_{XX})}{F_{ZZ} + 2F_{XX}} = 3(F_{ZZ} - F_{XX}) \tag{11}$$

Here, the packing has an initial anisotropy value between A = 0.02-0.05 at the end of the compaction phase. This value is insignificant compared to the anisotropy value of A = 0.26 in the 3D-DEM polyhedron model of Toyoura sand prepared under gravity and X-ray tomography of laboratory sand samples on Hostun sand prepared by the air pluviation method in (Mohamed et al. 2022) and (Wiebicke et al. 2020) respectively.

In terms of void ratio, its initial value is controlled by changing the friction coefficient during the compaction and no equality is sought between the DEM model void ratio and the real soil void ratio. Indeed, for the same mechanical behavior obtained after calibration (see below), the DEM sample will be shown to conform a lower void ratio value, which can be explained by the fact that the DEM void ratio does not account for the intra-aggregate pores that exist in the aggregated silty clay particles of tropical soils as shown in Fig. 3, and which actually justify the previous choice of a lower E_{mod} value for the fine contacts. On the other hand, the model will be calibrated for a specific void ratio value and a proportionality between the laboratory and model void ratios will be efficiently used throughout the manuscript as shown in Table 1, directly switching from the real soil void ratio to the one of DEM samples through a multiplicative coefficient that is defined within the calibration phase in the next section. While this idea shares some similarities with the consideration of a common relative density between lab samples and DEM packings, e.g. (Salot et al. 2009; Angelidakis et al. 2021), it is somewhat simpler since it does not require the definition of minimum and maximum void ratios in the DEM.

Also, during the subsequent triaxial shearing phase, the quasi-static condition is assured by the following condition of the inertial number $I_r \leq 10^{-4}$.

PARAMETRIC STUDY AND MODEL CALIBRATION

Effects of different coarse and fine mixtures

The role of the considered contact mixture in the model is first illustrated by performing a drained triaxial simulation in three different cases that will adopt respectively the mixture or just one kind of contact (model): either coarse or fine. Corresponding results are shown in Fig. 7, together with experimental data obtained by Mouali et al. (2019) for the tropical soil at hand. As expected, the results show that the model exhibits a greater contraction behavior for the sample with only fine contacts, while the sample with mixed contacts falls somewhere in between the two extreme cases. As for the deviatoric vs axial strain curve, the sample with only coarse contacts shows a stiffer behavior and a higher maximum deviatoric stress than the other samples. In addition, that sample with only coarse contacts shows a dilation tendency starting from an axial strain value $\epsilon_a \approx 11\%$ which is not the case for the experimental data. The sample with only fine contacts, on the other hand, exhibits very soft behavior in the $q - \epsilon_a$ curve and purely contracting behavior in the $\epsilon_v - \epsilon_a$ curve. Finally, the sample with a contacts mixture shows a very good agreement with the experimental data. The existence of fine contacts in the mixed sample has a greater effect on the volumetric strain behavior than on the stiffness and deviatoric response as shown in Fig. 7, indicating the importance of the fine contacts in capturing the tropical soil's continuous contraction volumetric response for these loading conditions. While the DEM simulations are here stopped at an axial strain value $\epsilon_a = 20\%$ as a limit being consistent with the experimental data, a similar mixture case will be presented until $\epsilon_a = 50\%$ in Fig. 13 within a subsequent parametric study and confirm that volumetric behavior.

Also, the evolution of the coordination numbers Z^{Coarse} or Z^{Fine} (average number of coarse or fine contacts per particle) and mechanical coordination numbers $Z^{Coarse}_{mechanical}$ and $Z^{Fine}_{mechanical}$ for the coarse and fine contact networks (average number of coarse or fine contacts per stress-transmitting particle) are used to obtain more insights in the DEM sample:

$$Z^{Coarse} = \frac{2N_c^{Coarse}}{N_t} \quad \text{and} \quad Z^{Fine} = \frac{2N_c^{fine}}{N_t} \tag{12}$$

$$Z^{Coarse}_{mechanical} = \frac{2N_c^{Coarse}}{N_t - N_r} \quad \text{and} \quad Z^{Fine}_{mechanical} = \frac{2N_c^{fine}}{N_t - N_r} \tag{13}$$

where N_c^* denotes the number of contacts of a specific type and N_t and N_r are the total number of particles and rattlers (showing 0 or 1 contact of any type), respectively. From a micro-scale point of view, it is noted from Fig. 8 that the initial (pre-shearing) percentage of the fine contacts in the mixture case is higher than the one of coarse contacts and represents 71% of the total number, which is consistent with the presence of about 75% percent of clay and silt in the studied tropical soil, as shown in Fig. 1. The evolution of the $Z_{mechanical}$ for the two contact types in the mixed sample during the shearing phase shows a continuous increase in the number of fine contacts starting from $\epsilon_a = 3\%$ coinciding with a decrease in the number of coarse contacts (Fig. 9).

Effect of adhesive parameters F_0 and D_0

The effect of the adhesive component parameters F_0 and D_0 in Table 2 is next investigated. Three triaxial tests with different combinations of F_0 and D_0 are performed with confining pressure and the initial DEM void ratio equal to 100 kPa and 0.71, respectively. The results in Fig. 10 show that the values of F_0 and D_0 have an important role in the constitution of fine contacts during the preparation phase and significantly affect the evolution of fine contacts during the shearing phase. Also, the macroscopic results of the triaxial tests in Fig. 11 show that the volumetric behavior can be converted from contractive to dilative depending on the number of fine contacts in the sample, indicating an upward shift to the critical state line as a function of fine contacts. However, the F_0 and D_0 parameters have less effect on the $q - \epsilon_a$ curve which is consistent with the previous observation in Fig. 7.

On the other hand, the Fig. 12 compares the effect of different clay contents on the critical state line of tropical soils, using data from the Guadeloupe site and from (Futai et al. 2004) for tropical soils found in Ouro Preto, Southeast Brazil. Following the same methodology, as (Futai et al. 2004), the critical state line (CSL) is derived for Guadeloupe tropical soils using data from (Mouali et al. 2019; Suez Consulting 2016) for drained and undrained triaxial tests at a large axial strain $\epsilon_a = 25\%$ and essentially no change in the volumetric strain or pore pressure curves in the drained and undrained cases, respectively. Sometimes critical state conditions could not be achieved, and data close to critical state conditions was used. The analysis of the experimental results in Fig. 12 shows that the CSL is very sensitive to the different soil mixtures. The CSL tends to move downwards on the $e - p'$ plane as sand or silt content increases relative to clay content, which is consistent with the previous DEM results in Fig. 11 about the shift in DEM CSL caused by the number of fine contacts.

Evolution of fabric tensor and effect of rolling resistance parameter of fine contacts

In this section, the effect of the rolling resistance parameter of fine contacts is studied by performing two triaxial tests with different values of μ_r=0.37 and 0.05 for that contact phase. Also, the evolution of the fabric tensor for the coarse and fine particles is observed until a large axial strain value $\epsilon_a = 50\%$. The results in Fig. 13 show that the μ_r parameter of fine contact has a limited effect on the deviatoric stress until $\epsilon_a = 25\%$. Then, at a larger axial strain value, the deviatoric stress is affected by changing the value of the μ_r which indicates that the critical state condition of the soil is influenced by the fine contacts. The evolution of the fabric tensor in Fig. 14 indicates once again that the coarse contact has a larger influence at the first stage of the test until $\epsilon_a = 10\%$ since the continuous network is essentially formed by coarse contacts (Fig. 2). At $\epsilon_a = 50\%$, the value of the anisotropy parameter A for the fine contacts is very close to the value of the total anisotropy, which confirms that the critical state is mainly determined by the fine contacts. Finally, Fig. 14 shows the force network at the end of one triaxial test which demonstrates that the main force network is at this stage no longer formed by coarse contacts only but that fine contacts now contribute heavily.

Model calibration

As it was shown above, the percentage of fine and coarse contact plays an important role in the mechanical behavior of the DEM model and is first calibrated, based on the previous parametric study of different mixtures and in agreement with the granulometry of the tropical soil studied. The rest of the model is then calibrated for one drained compression triaxial test by using a trial and error strategy, that applies to all other DEM model ingredients (contact parameters in Table 2 and the coefficient of proportionality between the void ratio of real soil and the DEM model in Table 1). Although we have calibrated the nine parameters of the two contact models from one drained triaxial test, we consider that a single drained triaxial test is sufficient for an efficient calibration since the fine contacts almost do not contribute to the stress-strain behavior (at least for the first stage of tests, until 25% of axial strain) as it is shown in Fig. 11. From the same figures, we can actually observe that the volumetric strain behavior of the mixture depends mainly on the fine contacts (amount of fine contacts + fine contact parameters). As it is shown clearly during the previous parametric study, this means that different contact types influence deviatoric stress and volumetric strain in an almost uncoupled fashion and this is the reason why the mechanical behavior of this type of soil is very special. This feature of the soil makes it easier to obtain calibration parameters from just one drained triaxial test and the robustness of that calibration will be furthermore checked through blind predictions in a subsequent validation step.

VALIDATION OF THE DEM MODEL UNDER DIFFERENT LOADING CONDITIONS

In the next sections, the model will be validated under oedometer tests and different drained and undrained monotonic and cyclic loadings.

Oedometer Test

In this section, the prediction of the DEM model for one-dimensional compression tests is assessed. Two experimental oedometer tests (Mouali 2021) are considered as references, for remolded samples of tropical soils with different initial void ratio values: 1.06 and 1.51, as shown in Fig. 15. In DEM, no strictly adequate packing (i.e., with a void ratio scaled by the calibrated proportionality factor 1.6) could be created for the loosest case, unlike for the densest one, and the discussion will only be qualitative for that test. It is worth mentioning that the numerical and experimental tests are compared up to a maximum mean pressure p' = 3 MPa. Beyond this value, an excessive overlap at fine contacts in the DEM and particle-crushing phenomenon in experiments would invalidate the DEM model results. However, the behavior of this soil under excessively high pressure is beyond the scope of this study.

In this framework, the DEM model results are shown to be coherent with the experimental data in Fig. 15. First, both the experimental data and the DEM have close slopes for the loading-unloading line (elastic swelling) and the normal consolidation line. Second, for the DEM model, the degree of over-consolidation OCR increases as the initial void ratio decreases, which is consistent with the experimental data. Furthermore, the DEM model offers a reasonable evolution for the K_0 coefficient during the over-consolidated stage when compared to the behavior observed in the literature, for example, in (Lee et al. 2013) in which the K_0 value for the over-consolidated sample is higher than the K_0 value for the normally consolidated sample.

Drained Triaxial Tests

Fig. 16 presents the model's prediction together with experimental results from (Mouali et al. 2019) for three drained triaxial tests with an initial DEM void ratio e = 0.71 in Table 1 and different confining pressures. Three intermediate loading-unloading cycles are shown in the simulations that are not present in the experimental data. The simulation results for both the deviatoric $q - \epsilon_a$ and $\epsilon_a - \epsilon_v$ curves show very good agreement with the experimental data, indicating the model's capability in following the strongly nonlinear behavior of the tropical soil in the $q - \epsilon_a$ curve at various stages of the tests, such as initial slope and maximum strength under different confining pressure values. Also, the model can capture the continuous contraction behavior of the tropical soil until a relatively high axial strain value $\epsilon_a = 14\%$.

Undrained Triaxial Tests

Further investigations for the model predictions under monotonic loading are carried out by considering an undrained condition (constant volume) for the triaxial compression. As shown in Table 1, the predictions are tested for two different void ratios, with various confining pressures

(100, 300 and 510 kPa) in each case (Suez Consulting 2016).

Again, the simulations in Fig. 17 and Fig. 18 illustrate a good agreement with the experiments on the curves of $q - p'$ and $q - \epsilon_a$ for the different confining pressures and different void ratios. First, the DEM model and the real soil have nearly identical strength envelops and critical state lines in the $q - p'$ plane $M = q/p'$. Second, the numerical results in $q - \epsilon_a$ have a very close slope and softening regime to the experimental data. We emphasize here that the DEM model can directly capture the influence of the different void ratio values on the undrained results (different contractive or dilative behaviors) through the straightforward proportional definition of the DEM void ratio with respect to soil void ratio (Table 1).

Finally, because the numerical and experimental data for the drained and undrained tests are nearly identical at the final stages of the $\epsilon_v - \epsilon_a$ and $q - p'$ curves, the numerical results suggest that the DEM model shares similar CSL datapoints as the real soil in the $e - p'$ plane with a shifting parameter equal to the proportionality coefficient in Table 1.

Cyclic Undrained Triaxial Test With Different Strain Amplitudes

The DEM model prediction and the experimental data (Mouali 2021) of three undrained cyclic triaxial tests for initial p' = 100 kPa are presented in Fig. 19. Each test comprises 50 cycles with a constant amplitude in axial strain among (0.2%, 0.5% and 1%) and may serve to assess the liquefaction ability of the tropical soil. The performance of the DEM model shows a good agreement with the experimental data at different cyclic amplitudes. In general, more strength degradation is observed by increasing the cyclic strain amplitude and by increasing the number of cycles.

On the other hand, Fig. 20 shows the evolution of the deviatoric stress as a function of the effective mean pressure for the case of a strain amplitude = 1%. By increasing the number of cycles, a continuous decrease in effective mean pressure is observed. Also, the maximum mean pressure is observed on the extension side coherently with the experimental data. Finally, the DEM model gives a very close qualitative prediction of the experimental data at different stages of the test. For example, at the start of the test, both the experimental data and the model show a faster rate of decrease of the effective mean pressure and the decreasing rate becomes slower as the number of cycles increases. It is remarkable that the DEM can reproduce such an evolving behavior during cyclic loading with a very limited number of parameters, if one compares it to a phenomenological approach, e.g. the elasto-plastic model by Duriez and Vincens (2015) with 17 independent parameters.

CONCLUSION

This article presents a quantitative application of the DEM approach to a complex in-situ tropical soil which contains different types of soil among sand, silt and clay. A 3D-DEM model is developed with simple spherical particles conforming a wide size distribution to allow small particles to occupy the void and to form local force networks between the large particles, i.e., the main skeleton. Two different contact models are assigned to represent the different physics existing within tropical soil's coarse or fine components. The linear rolling resistance contact model is used to represent the coarse component and the adhesive rolling resistance contact model is used for the fine and cohesive component. The latter contact model simulates cohesion by introducing a linear approximation of the van der Waals attraction force, characterized by a maximum attraction force and a maximum gap distance.

The parametric study performed on the effect of the adhesive parameters F_0 and D_0 reveals the important effect of these parameters on the number of fine contacts during the preparation and shearing phases. For the same initial void ratio, more dilative behavior is observed by increasing the number of fine contents implying an upward shift for CSL in the $e - p'$ plane with increasing the number of fine contacts. These numerical results are consistent with the analysis of the effect of clay contents on the CSL of tropical soils. Also, the parametric study on the effect of using different mixtures highlights that the coarse contacts have more influence on the deviatoric stress curve however fine contacts impact more the volumetric strain behavior. In addition, the evolution of the fabric anisotropy shows that the coarse contacts control the mechanical behavior of the soil during the first stage of a triaxial test until $\epsilon_a \approx 25\%$ whereas, near the critical state, the behavior is highly impacted by the composition of fine contacts.

After a parametric study on the effects of using such a numerical mixture, the model is calibrated for a drained triaxial test with a specific void ratio. The calibration result agrees very well with the experimental data of tropical soils. For other tests, a proportionality between the real soil void ratio and the DEM model void ratio is proposed to obtain equivalent mechanical behaviors. The proportionality coefficient is shown to be effective during the validation phase for a wide range of void ratios and different stress paths.

The validation of the DEM model for drained, undrained triaxial (constant volume) and oedometer tests at various confining pressure and void ratio values shows a high level of agreement with the experimental results. Furthermore, the validation of the model under undrained triaxial cyclic tests shows a remarkable agreement with the experimental data at different cyclic strain amplitudes for the stress-strain and deviatoric-effective mean stress curves.

As for the limitations of the proposed DEM approach, in addition to the absence of the grain-crushing phenomenon, the use of soft contacts to simulate silty clay aggregates could lead to excessive elastic deformation and biased unloading behavior under very high mean pressure, rendering the model invalid under those conditions.

Still, this 3D-DEM model could be used within a multi-scale, hierarchical, modeling approach to efficiently assess the structural behavior of earth dams built, or under construction, in tropical areas, being for instance provided that structure dimensions lead to moderate confining pressures being compatible with the present study.

DATA AVAILABILITY STATEMENT

Some or all data, models, or codes that support the findings of this study are available from the corresponding author upon reasonable request.

ACKNOWLEDGEMENTS

The authors would like to express their sincere thanks and gratitude to the Itasca Educational Partnership Program (IEP, Zhao Cheng and Sacha Emam) for their valuable support and for providing PFC software, to SUEZ-SAFEGE for the funding of the PhD associated with this article and for providing the data for the considered construction site, and to ANTEA Group (Lila Mouali) for providing raw experimental data.

REFERENCES

Angelidakis, V., Nadimi, S., Otsubo, M., and Utili, S. (2021). "CLUMP: A code library to generate universal multi-sphere particles." *SoftwareX*, 15, 100735.

Duriez, J. and Bonelli, S. (2021). "Precision and computational costs of Level Set-Discrete Element Method (LS-DEM) with respect to DEM." *Computers and Geotechnics*, 134, 104033.

Duriez, J. and Vincens, É. (2015). "Constitutive modelling of cohesionless soils and interfaces with various internal states: An elasto-plastic approach." *Computers and Geotechnics*, 63, 33–45.

Futai, M. and Almeida, M. (2005). "An experimental investigation of the mechanical behaviour of an unsaturated gneiss residual soil." *Géotechnique*, 55(3), 201–213.

Futai, M., Almeida, M., and Lacerda, W. (2004). "Yield, strength, and critical state behavior of a tropical saturated soil." *Journal of Geotechnical and Geoenvironmental Engineering*, 130(11), 1169–1179.

Gilabert, F., Roux, J.-N., and Castellanos, A. (2007). "Computer simulation of model cohesive powders: Influence of assembling procedure and contact laws on low consolidation states." *Physical review E*, 75(1), 011303.

Gong, J., Wang, X., Li, L., and Nie, Z. (2019). "Dem study of the effect of fines content on the small-strain stiffness of gap-graded soils." *Computers and Geotechnics*, 112, 35–40.

Gu, X., Zhang, J., and Huang, X. (2020). "Dem analysis of monotonic and cyclic behaviors of sand based on critical state soil mechanics framework." *Computers and Geotechnics*, 128, 103787.

Gu, Y., Ozel, A., and Sundaresan, S. (2016). "A modified cohesion model for cfd–dem simulations of fluidization." *Powder technology*, 296, 17–28.

Hattab, M. and Fleureau, J.-M. (2011). "Experimental analysis of kaolinite particle orientation during triaxial path." *International Journal for Numerical and Analytical Methods in Geomechanics*, 35(8), 947–968.

Hosn, R. A., Sibille, L., Benahmed, N., and Chareyre, B. (2017). “Discrete numerical modeling of loose soil with spherical particles and interparticle rolling friction.” *Granular matter*, 19(1), 4.

Itasca (2018). *PFC — Particle Flow Code, Ver. 6.0.* Itasca Consulting Group, Inc.

Karapiperis, K., Marshall, J. P., and Andrade, J. E. (2020). “Reduced gravity effects on the strength of granular matter: DEM simulations versus experiments.” *Journal of Geotechnical and Geoenvironmental Engineering*, 146(5), 06020005.

Lee, J., Yun, T. S., Lee, D., and Lee, J. (2013). “Assessment of k0 correlation to strength for granular materials.” *Soils and foundations*, 53(4), 584–595.

Li, T., Jiang, M., and Thornton, C. (2018). “Three-dimensional discrete element analysis of triaxial tests and wetting tests on unsaturated compacted silt.” *Computers and Geotechnics*, 97, 90–102.

Lopes, B. d. C. F. L., Kühn, V. d. O., Queiroz, Â. C. G., Caicedo, B., and Neto, M. P. C. (2022). “Structure evaluation of a tropical residual soil under wide range of compaction conditions.” *Géotechnique Letters*, 1–8.

Mendoza, C. and de Farias, M. M. (2020). “Critical state model for structured soil.” *Journal of Rock Mechanics and Geotechnical Engineering*, 12(3), 630–641.

Mohamed, T., Duriez, J., Veylon, G., and Peyras, L. (2022). “DEM models using direct and indirect shape descriptions for Toyoura sand along monotonous loading paths.” *Computers and Geotechnics*, 142, 104551.

Mouali, L. (2021). “Experimental and analytical study of the hydromechanics of residual tropical soils: application to the numerical modelling of an earthfill dam in french west indies under seismic loading.” Ph.D. thesis, University of Aix-Marseille, France, (in French).

Mouali, L., Antoinet, E., Dias, D., Veylon, G., Duriez, J., and Peyras, L. (2019). “Seismic analysis of an earth dam in a tropical geologic context.” *7th International Conference on Earthquake Geotechnical Engineering*, Rome, Italy, CRC Press, 8, <https://hal.inrae.fr/hal-02609700> (June).

Potyondy, D. O. and Cundall, P. (2004). “A bonded-particle model for rock.” *International journal of rock mechanics and mining sciences*, 41(8), 1329–1364.

Salot, C., Gotteland, P., and Villard, P. (2009). “Influence of relative density on granular materials behavior: Dem simulations of triaxial tests.” *Granular Matter*, 11(4), 221–236.

Shire, T., O’Sullivan, C., and Hanley, K. (2016). “The influence of fines content and size-ratio on the micro-scale properties of dense bimodal materials.” *Granular Matter*, 18(3), 1–10.

Sibille, L., Villard, P., Darve, F., and Aboul Hosn, R. (2019). “Quantitative prediction of discrete element models on complex loading paths.” *International Journal for Numerical and Analytical Methods in Geomechanics*, 43(5), 858–887.

Suez Consulting (2016). “Technical report 12MGU036 (in french), by T. Gaillard, G. Dias Omonte, B. Lauzier and S. Bonnet.

Sun, R., Xiao, H., and Sun, H. (2018). “Investigating the settling dynamics of cohesive silt particles with particle-resolving simulations.” *Advances in Water Resources*, 111, 406–422.

Tsuji, T., Nakagawa, Y., Matsumoto, N., Kadono, Y., Takayama, T., and Tanaka, T. (2012). “3-d dem simulation of cohesive soil-pushing behavior by bulldozer blade.” *Journal of Terramechanics*, 49(1), 37–47.

Wang, R., Fu, P., Zhang, J.-M., and Dafalias, Y. F. (2016). “Dem study of fabric features governing undrained post-liquefaction shear deformation of sand.” *Acta Geotechnica*, 11(6), 1321–1337.

Wiebicke, M., Andò, E., Viggiani, G., and Herle, I. (2020). “Measuring the evolution of contact fabric in shear bands with x-ray tomography.” *Acta Geotechnica*, 15(1), 79–93.

Yang, J. and Liu, X. (2016). “Shear wave velocity and stiffness of sand: the role of non-plastic fines.” *Géotechnique*, 66(6), 500–514.

List of Tables

TABLE 1. Real tropical soil and DEM void ratio values for different simulations

	initial void ratio (e)	void ratio (e)	void ratio (e)
Simulation	Drained triaxial	Undrained triaxial	Undrained cyclic triaxial
Real soil	1.12	1.07-1.312	1
DEM model	0.71	0.66-0.82	0.62

TABLE 2. DEM parameters for the different contact models

Contact model	Contact						Packing			
	E_{mod} (MPa)	K_n/K_s (-)	μ (-)	μ_r (-)	D_0 (mm)	F_0 (N)	D_{min} (mm)	D_{max}/D_{min} (-)	N_b (-)	Initial A (-)
Linear rolling resistance for coarse network	370	1	0.4	0.7	-	-	4	10	5100	0.02-0.05
Adhesive model for fine network	30	1	0.4	0.37	0.5	1.5				

List of Figures

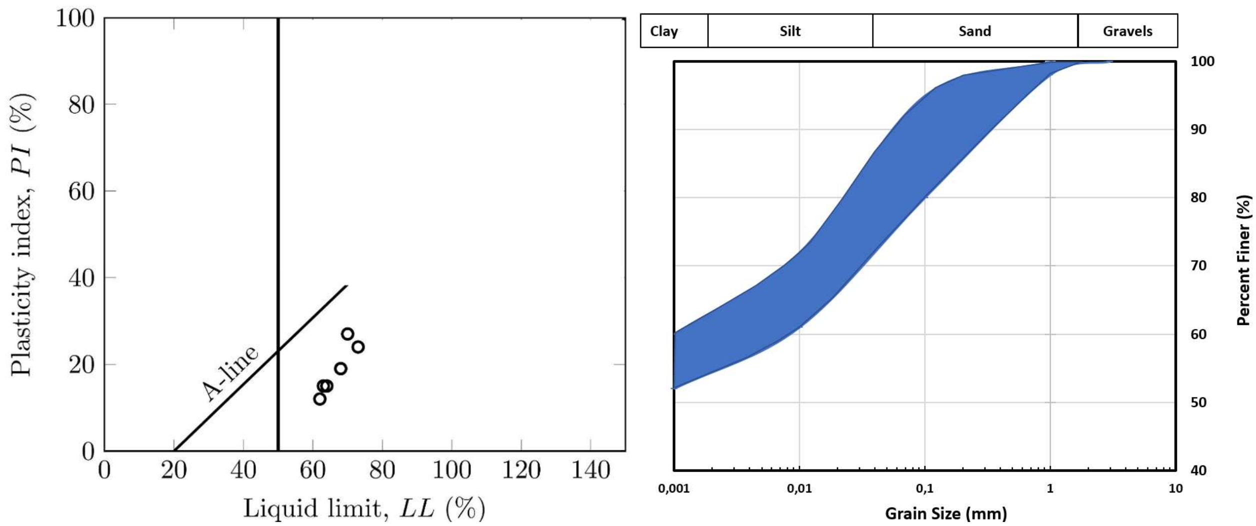

Fig. 1. The plasticity chart and particle size distribution (envelope of six different samples) of the tropical soil samples used in this study and collected from an earth dam construction site in Guadeloupe, France (Mouali 2021).

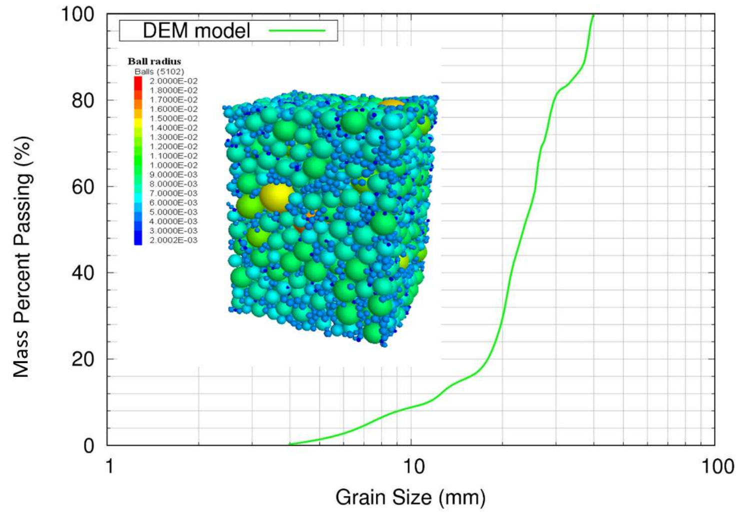

Fig. 2. Particle size distribution of the proposed 3D-DEM model (itself in the inset, where different colors correspond to different radii) for tropical soil.

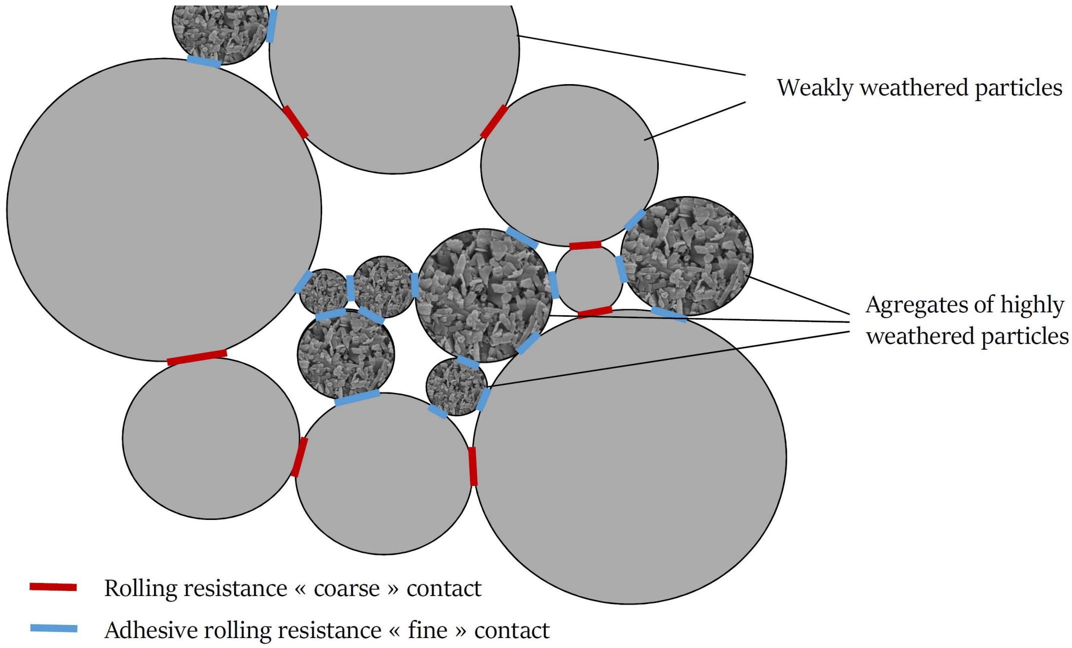

Fig. 3. Micro-scale interpretation of using different contact models in the DEM. The so-called coarse DEM contacts correspond to the soil's granular components, whereas the so-called fine contacts account for much smaller silty clay solid particles and intra-aggregate pores.

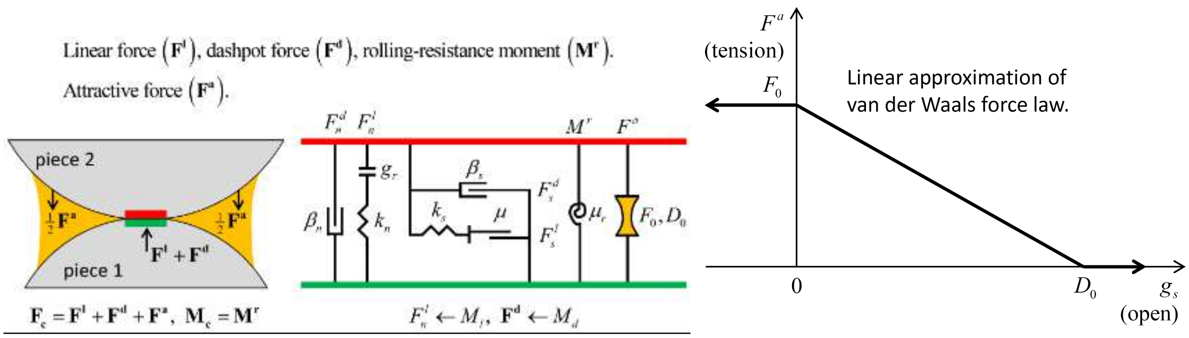

Fig. 4. Adhesive rolling resistance contact model and van der Waals approximation for attraction force vs gap distance between particles (Itasca 2018).

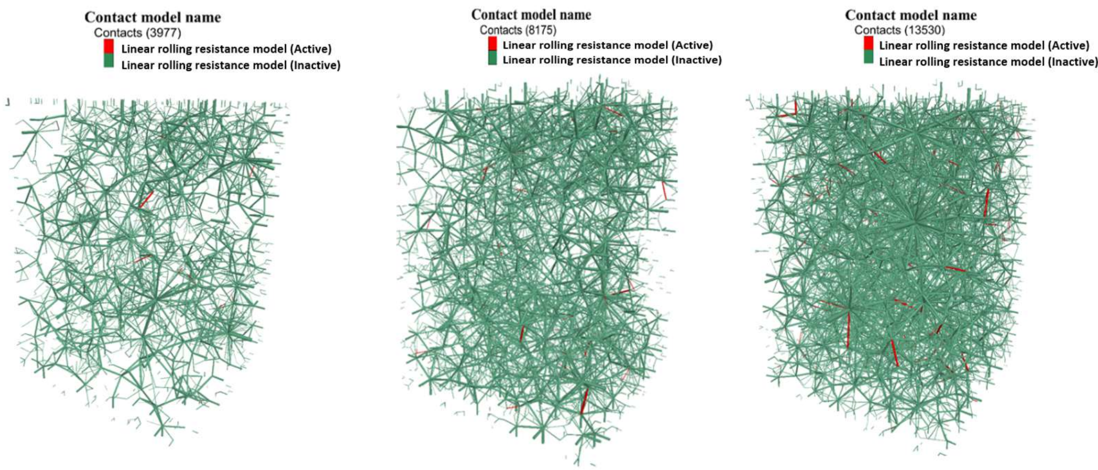

Fig. 5. Visualization of all possible particle pairs serving to describe the coarse component of the soil, as defined during the initial preparation stage. The maximum possible coordination number Z in that "coarse contacts" phase is variable (increasing from left to right) and is controlled by a numerical parameter defining the very initial stage of the packing (through overlap considerations, see text).

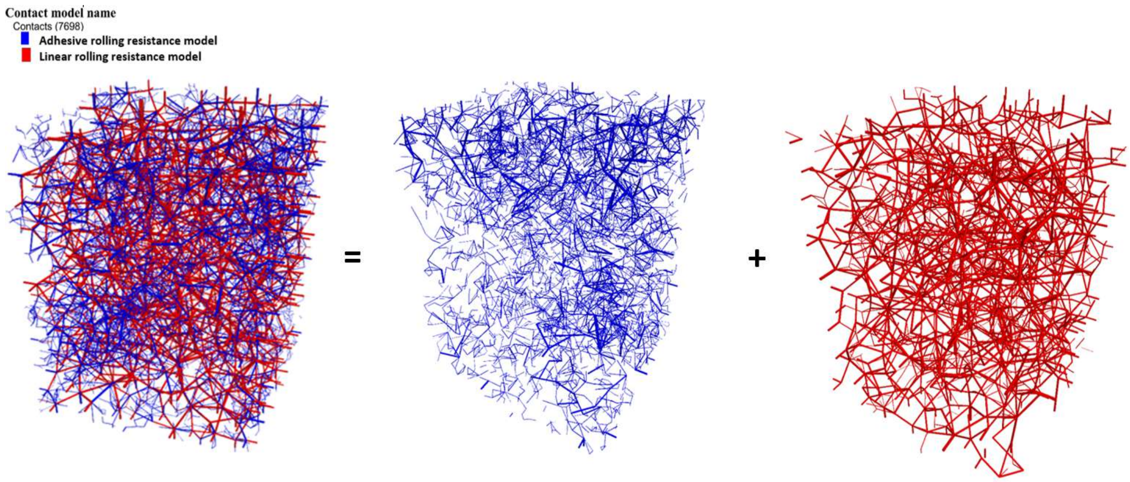

Fig. 6. The fine (in blue) and coarse (in red) contact networks of a sample with an initial confining pressure = 100 kPa and an initial void ratio = 0.71 in Table 1. The force network of the coarse contacts is more continuous and represents the main skeleton of the sample, whereas, the fine contacts represent the local force network between the coarse contacts.

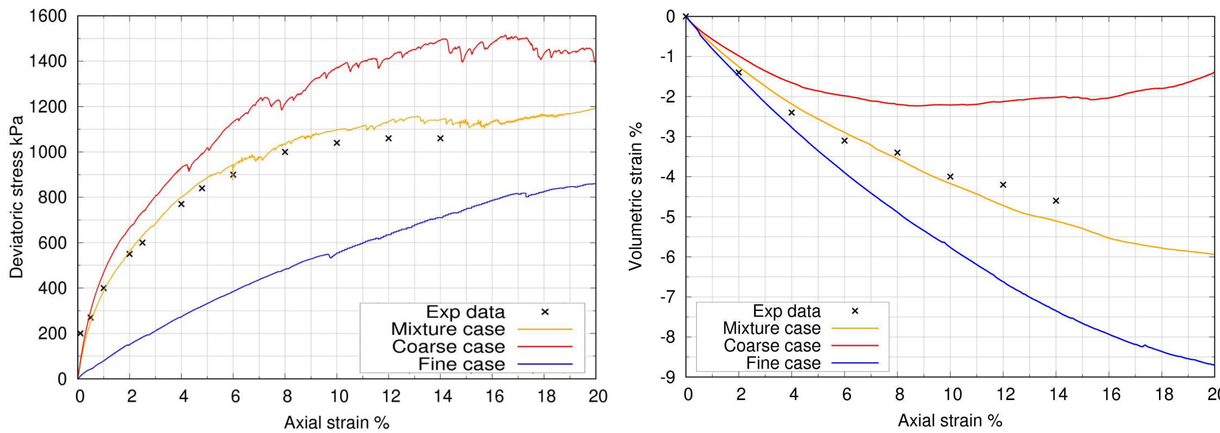

Fig. 7. The effect of using a contact mixture on the mechanical response for a drained triaxial test with confining pressure 535 kPa and a DEM initial void ratio e = 0.71 equivalent to the experimental one (see Table 1). Experimental data from (Mouali et al. 2019).

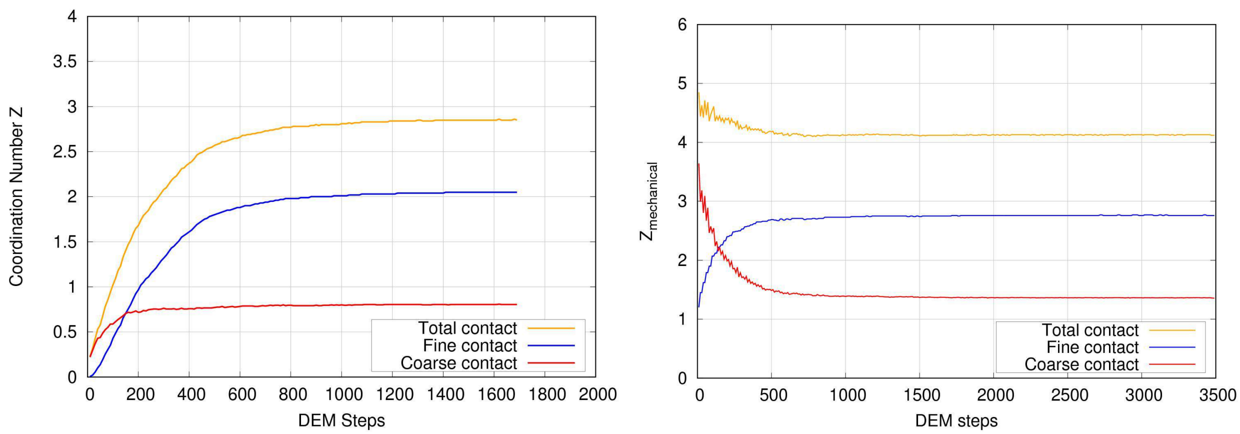

Fig. 8. Evolution of the coordination number Z and mechanical coordination number $Z_{mechanical}$ for the various contact types in the mixed sample of Fig. 7 during a preparation phase towards a final p'= 535 kPa and DEM void ratio = 0.71.

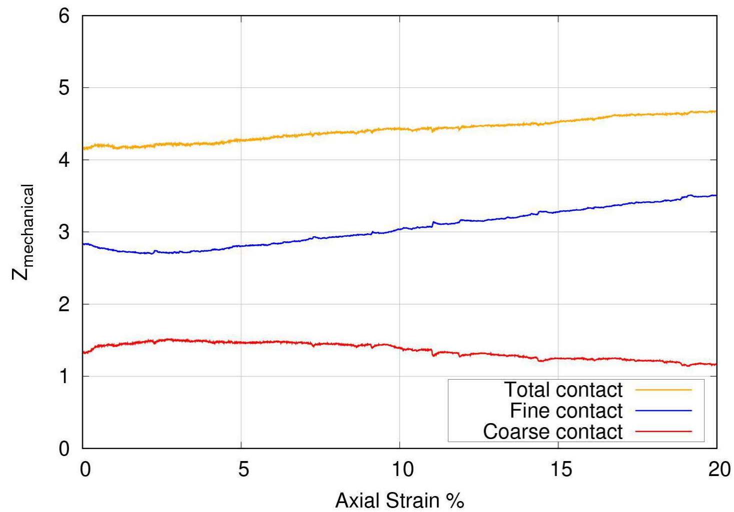

Fig. 9. Evolution of the mechanical coordination number $Z_{mechanical}$ for the various contact types in the mixed sample of Fig. 7 during the shearing phase with confining pressure 535 kPa and a DEM initial void ratio e = 0.71.

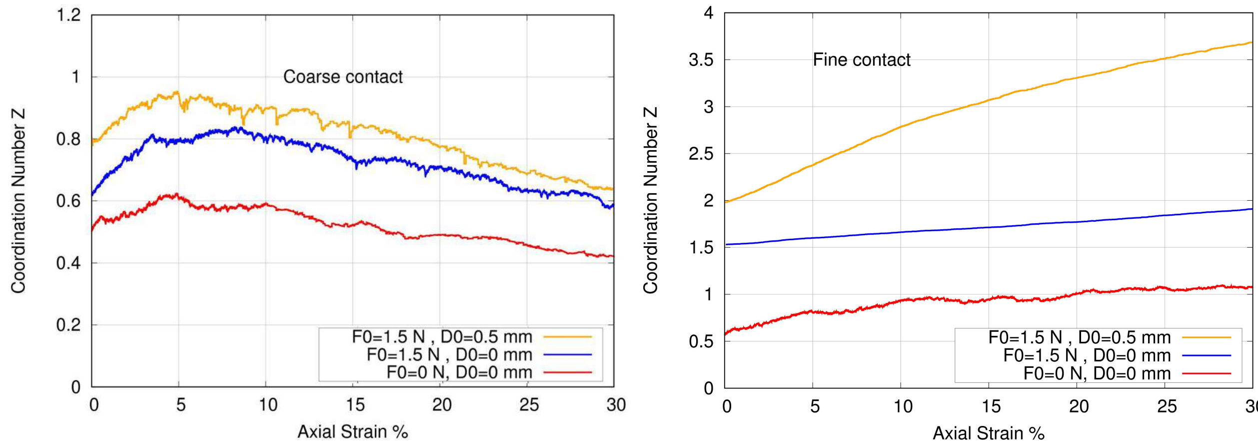

Fig. 10. The evolution of the coarse and fine contacts for the DEM model with different combinations of F_0 and D_0 during drained triaxial tests with confining pressure = 100 kPa for a DEM void ratio e = 0.715.

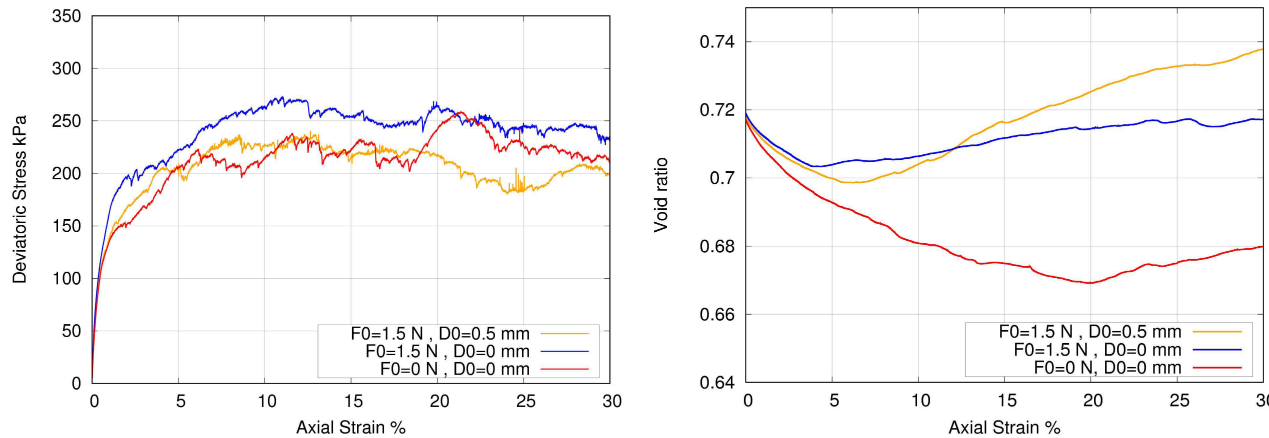

Fig. 11. DEM model results for different combination of F_0 and D_0 under a drained triaxial test with confining pressure = 100 kPa for a DEM void ratio e = 0.715.

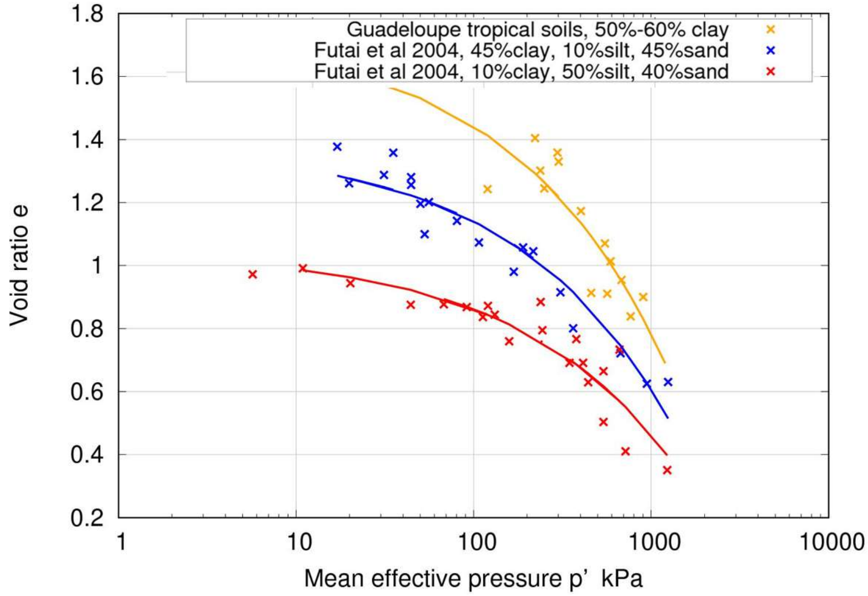

Fig. 12. Different critical state lines for different tropical soils with different clay contents. Solid lines represent the best-fitting model for the different soils.

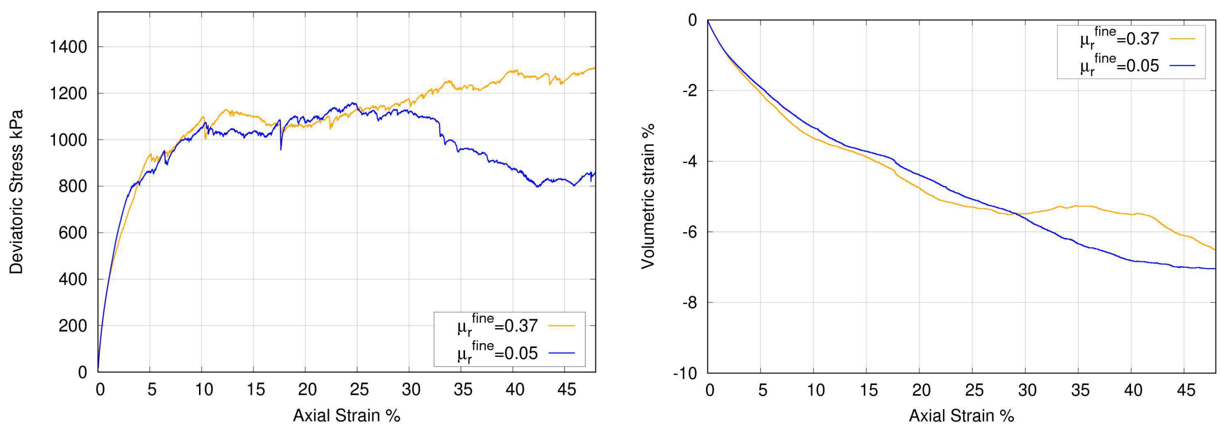

Fig. 13. The effect of the rolling resistance parameter of fine contacts μ_r^{fine} on the mechanical response for a drained triaxial test with confining pressure 535 kPa and a DEM initial void ratio e = 0.71

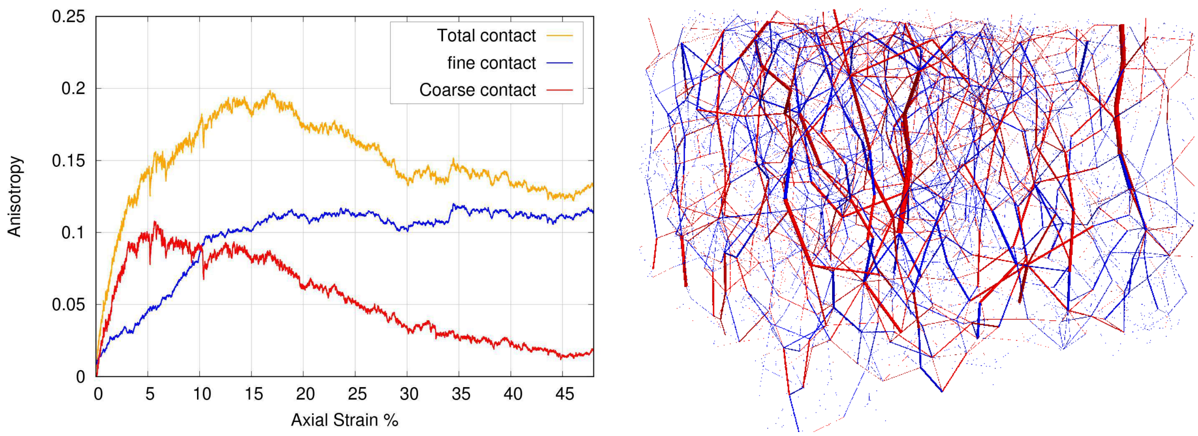

Fig. 14. Left: the evolution of fabric for the coarse and fine contacts for a drained triaxial test with 535 kPa confining pressure, initial DEM void ratio = 0.71 and μ_r^{fine}=0.37. Right: the force network at ϵ_a = 50% (blue is fine contacts and red is coarse contacts) and the size of cylinders represents the force magnitude.

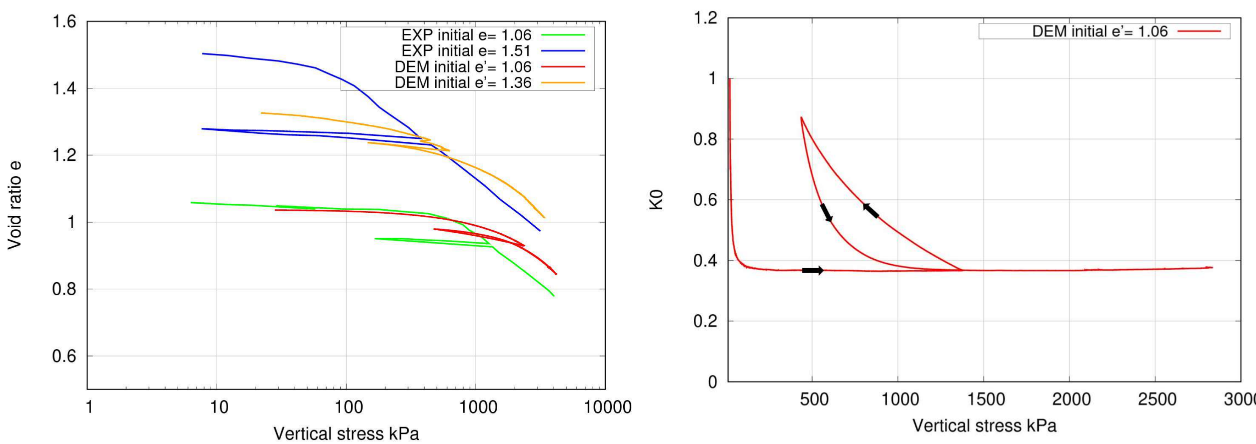

Fig. 15. Left: DEM model prediction for two oedometer tests vs experimental data from (Mouali 2021). Right: evolution of $k_0 = \sigma_h/\sigma_v$ coefficient during one oedometer test with one unloading-reloading cycle.

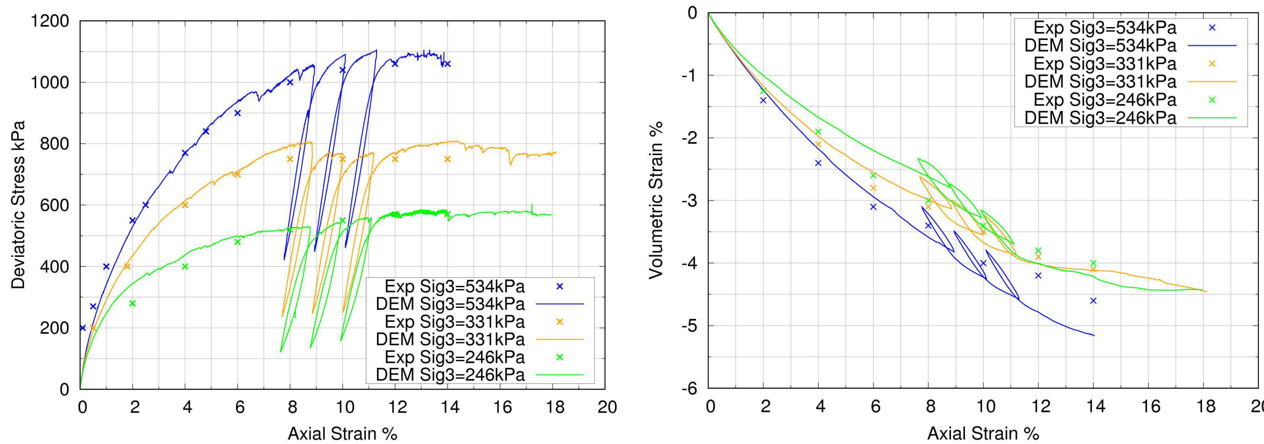

Fig. 16. DEM model validation under different drained triaxial tests with different confining pressure values including one calibration curve for confining pressure = 535 kPa for a DEM void ratio e = 0.71, see Table 1. Experimental data from (Mouali et al. 2019).

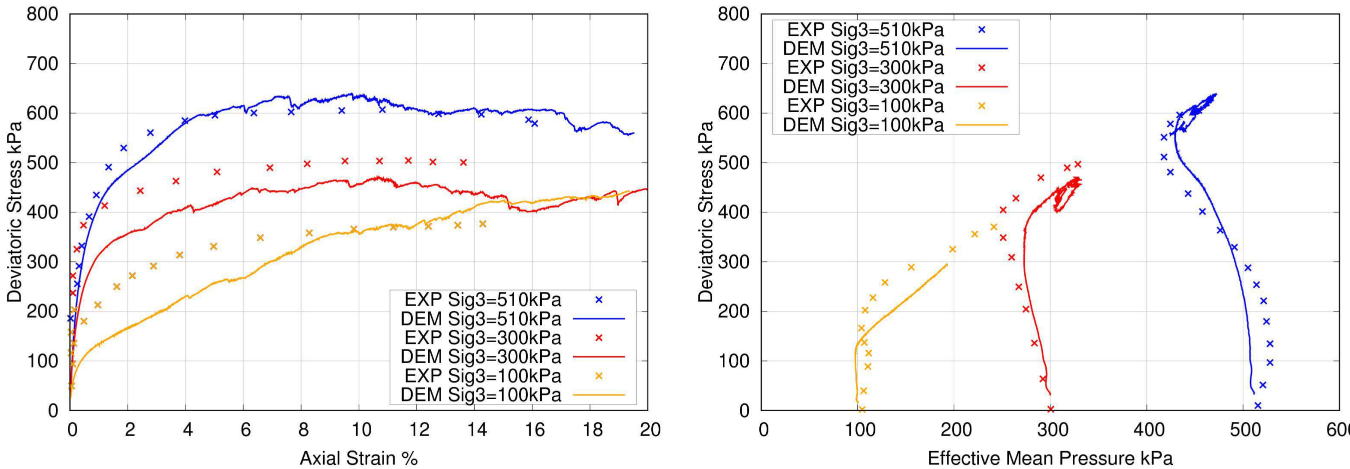

Fig. 17. DEM model predictions for the undrained triaxial condition and a DEM void ratio e = 0.69, see Table 1. Solid lines are simulations and points are the experimental data from (Suez Consulting 2016).

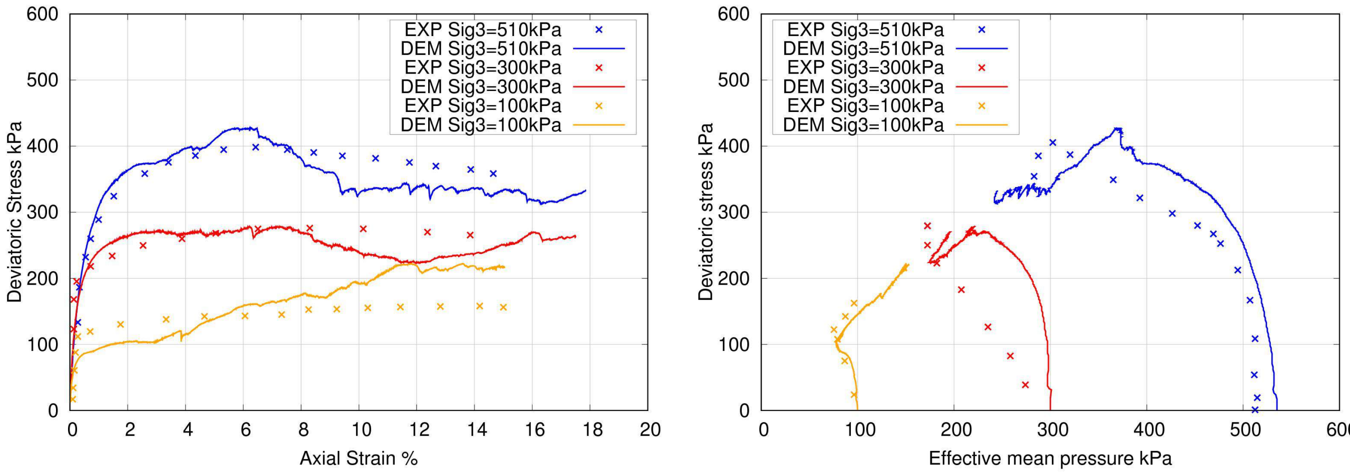

Fig. 18. DEM model predictions for the undrained triaxial condition and a DEM void ratio e = 0.82, see Table 1. Solid lines are simulations and points are the experimental data from (Suez Consulting 2016).

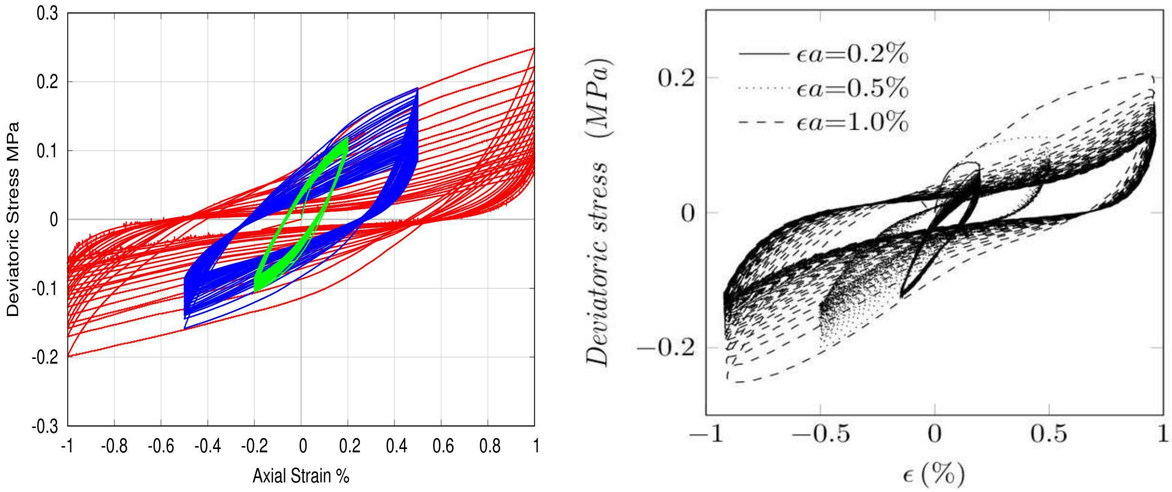

Fig. 19. DEM model predictions for undrained cyclic triaxial tests with different strain cyclic amplitudes (0.2%,0.5% and 1%) under confining pressure = 100 kPa for 50 cycles. Left: DEM model and right: experimental data from (Mouali 2021).

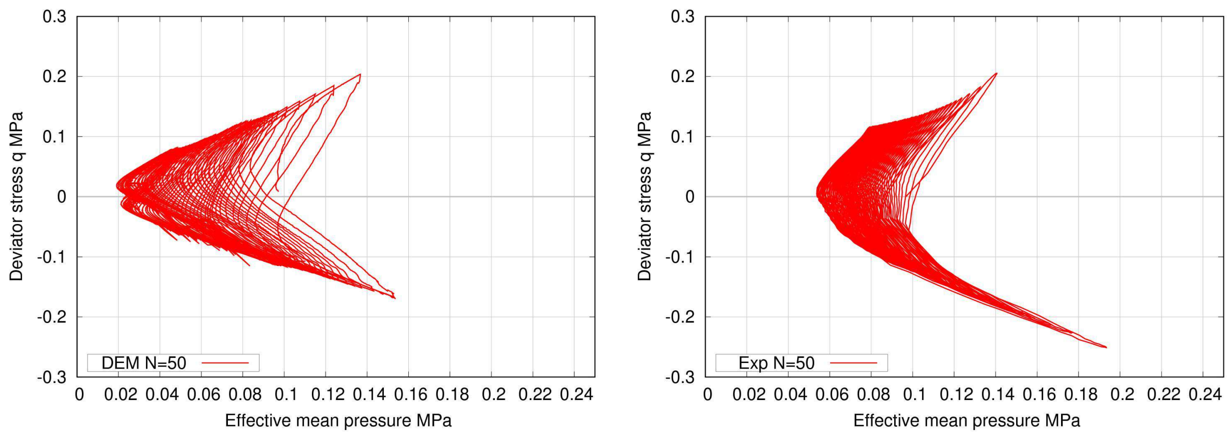

Fig. 20. Deviatoric stress versus effective pressure for the test with strain cycle amplitude = 1% for 50 cycles. Left: DEM model and right: experiments (Mouali 2021).